Differential Outcome between BALB/c and C57BL/6 Mice after *Escherichia coli* O157:H7 Infection Is Associated with a Dissimilar Tolerance Mechanism

Alan M. Bernal,[a] Romina Jimena Fernández-Brando,[a] Andrea Cecilia Bruballa,[a] Gabriela A. Fiorentino,[a,b] Gonzalo Ezequiel Pineda,[a]
Elsa Zotta,[c] Mónica Vermeulen,[d] María Victoria Ramos,[a] Martin Rumbo,[e] Marina Sandra Palermo[a]

[a]Laboratorio de Patogénesis e Inmunología de Procesos Infecciosos, Instituto de Medicina Experimental (IMEX), Consejo Nacional de Investigaciones Científicas y Técnicas (CONICET)-Academia Nacional de Medicina, Buenos Aires, Argentina

[b]Laboratorio Central, Hospital Municipal del Niño de San Justo, Buenos Aires, Argentina

[c]Laboratorio de Fisiopatogenia, Departamento de Fisiología, Facultad de Medicina; Facultad de Farmacia y Bioquímica, Universidad de Buenos Aires, Buenos Aires, Argentina

[d]Laboratorio de Células Presentadoras de Antígenos y Respuesta Inflamatoria, IMEX CONICET-Academia Nacional de Medicina, Buenos Aires, Argentina

[e]Instituto de Estudios Inmunológicos y Fisiopatológicos-CONICET-Universidad Nacional de La Plata, La Plata, Argentina

ABSTRACT Enterohemorrhagic *Escherichia coli* (EHEC) infections can result in a wide range of clinical presentations despite that EHEC strains belong to the O157:H7 serotype, one of the most pathogenic forms. Although pathogen virulence influences disease outcome, we emphasize the concept of host-pathogen interactions, which involve resistance or tolerance mechanisms in the host that determine total host fitness and bacterial virulence. Taking advantage of the genetic differences between mouse strains, we analyzed the clinical progression in C57BL/6 and BALB/c weaned mice infected with an *E. coli* O157:H7 strain. We carefully analyzed colonization with several bacterial doses, clinical parameters, intestinal histology, and the integrity of the intestinal barrier, as well as local and systemic levels of antibodies to pathogenic factors. We demonstrated that although both strains had comparable susceptibility to Shiga toxin (Stx) and the intestinal bacterial burden was similar, C57BL/6 showed increased intestinal damage, alteration of the integrity of the intestinal barrier, and impaired renal function that resulted in increased mortality. The increased survival rate in the BALB/c strain was associated with an early specific antibody response as part of a tolerance mechanism.

KEYWORDS EHEC, intestinal infection, mouse model, defense mechanisms, antibodies, Shiga toxins

Enterohemorrhagic *Escherichia coli* (EHEC) include a diverse population of Shiga toxin (Stx)-producing *E. coli* that can cause illness in humans. There are important differences in epidemiology, transmission, and clinical characteristics of patients according to genetic variations in EHEC strains (1). In Argentina, as well as in other countries, *E. coli* O157:H7 is the most common EHEC serotype associated with the systemic complication hemolytic uremic syndrome (HUS) (2). Despite this, it is not clear why EHEC infections, even those caused by the O157:H7 strain, can result in a wide range of clinical presentations, from healthy carriers and watery diarrhea to HUS (1–3). Different outcomes in O157:H7-infected patients could reflect differences in health status, host tolerance/resistance, inflammatory response, anti-Stx or anti-LPS antibody titer, and/or genetic polymorphisms, among other factors (1–3).

Although virulence factors in the pathogen influence disease outcome (4), its ability to induce disease commonly depends on the context in which the microbe-host interaction takes place. In this regard, the biology of host-pathogen interaction determines

that bacteria and host genotypes and their interactions are responsible for pathogenicity (5–8).

Thus, the aim of this work was to contribute to the understanding of how host-pathogen interactions during EHEC infections cause disease in a percentage of individuals, while a large proportion of the same species not only has a favorable outcome, but also mounts protective immune responses.

Thus, taking advantage of the genetic differences between mouse strains, we analyzed the clinical progression in C57BL/6 (C57) and BALB/c mice infected with an O157:H7 strain belonging to clade 8. Since strains belonging to clade 8 have a greater capacity to adhere to epithelial cells and induce *in vivo* pathology, they are the most pathogenic EHEC group (4, 9, 10). We carefully analyzed colonization with several bacterial doses, clinical parameters, intestinal histology, and the integrity of the intestinal barrier, as well as local and systemic levels of antibodies against pathogenic factors. We chose the HUS model secondary to gastrointestinal infection by using weaned mice, due to their increased susceptibility compared to adults. We preferred this model over the antibiotic-treated or gnotobiotic mouse models, in which sensitivity of adult mice to EHEC infection is reached by the absence of competence with resident microbiota, as this is an important component of defense mechanisms against pathogens.

To reveal the role of genetic variation of mice in the defense mechanisms against O157:H7, we used the conceptual and analytical framework used during plant defense against parasites and herbivores (11), as well as animal host-parasite relationships (12). Through this point of view, defense mechanisms can be divided into tolerance and resistance. While resistance is the ability to limit microbial burden (i.e., to reduce O157:H7 colonization), tolerance is the ability to limit the disease severity or tissue damage induced by a certain pathogen burden (13).

C57 mice presented a worse outcome than BALB/c mice after infection with O157:H7 bacteria, leading to severe intestinal damage and epithelial barrier dysfunction, together with significant Stx-dependent renal damage and death in an increased percentage of mice. This different outcome after O157:H7 infection was not a consequence of an increased intestinal colonization or sensitivity to Stx in C57 mice, but rather a defense mechanism triggered in BALB/c mice that protected them from bacterial damage. In fact, BALB/c mice showed an early local production of IgA directed to the whole pathogenic bacteria, as well as systemic anti-Stx type 2 (Stx2) IgG. In addition, C57 mice treated with specific anti-Stx2 antibodies or sera from infected BALB/c mice obtained at 7 days postinfection survived the O157:H7 infection, confirming that the toxin is responsible for death. In addition, this result supports the hypothesis that specific antibodies can protect BALB/c mice.

This experimental approach allowed us to demonstrate that the kinetics of an appropriate and specific humoral immune response is a central point for distinguishing different host outcomes after the infection with O157:H7 strains, from healthy carriers to a benign and self-limited infection, or all the way to bloody diarrhea or HUS.

RESULTS

Survival rates and disease severity according to O157:H7 infective dose in C57 and BALB/c mice. Weaned specific-pathogen-free (SPF) C57 and BALB/c mice were gavaged with 2.8×10^{10} CFU of O157:H7. While all C57-infected animals died at 3 to 4 days postinfection (p.i.), most BALB/c mice ($\sim$80%) were alive at day 7 p.i. (Fig. 1A).

Disease severity after infection results from the balance between bacterial insult and anti-pathogen defense mechanisms, which classically include two components: resistance and tolerance (5–8). To analyze these components of defense, we tested disease severity by dividing mice in a binary manner as alive or dead according to their final outcome, along a range of infective doses ranging from 1.5 to 3.5×10^{12} CFU/kg of O157:H7. As observed in Fig. 1B and C, disease severity was relatively unaffected by increasing pathogen burden in both mouse strains, at least in the tested dose range, in such a way that while the great majority of BALB/c mice remained alive, the great
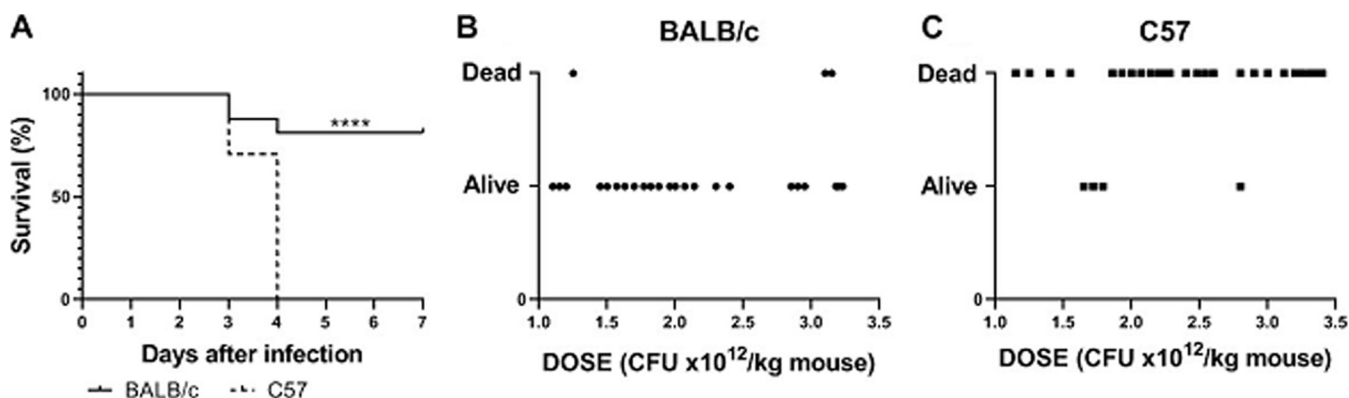
FIG 1 *In vivo* challenge with different infective doses of the O157:H7 strain. BALB/c and C57 mice were infected at the same time and immediately after weaning, as described in the Materials and Methods. The animals were observed daily until day 7, when survivors were euthanized. (A) High infective dose: 16 BALB/c and 17 C57 mice received 2.8×10^{10} CFU of O157:H7 in 3 independent experiments. The data were analyzed by log rank test; ****, $P < 0.0001$. (B) Dose-response curve in BALB/c mice; 27 BALB/c mice were challenged with different O157:H7 doses depicted as CFU/kg body weight and classified according to their outcome as alive or dead. (C) Dose-response curve in C57 mice. Same as in (B); $n = 34$. Data in figures (B) and (C) were analyzed by exact Fisher's test. Difference between mouse strains: ****, $P < 0.0001$.

majority of C57 mice died at 4 days p.i. These results suggest that BALB/c mice were able to manage O157:H7 infection by maintaining a better health status than C57 mice.

Clinical and biochemical parameters in C57 and BALB/c mice infected with O157:H7. Death after infection is associated with Stx2-dependent clinical signs, including weight loss, morbidity, and increased plasma urea levels (14–18). While C57 mice exhibited increased plasma urea levels compatible with Stx2-induced renal injury at day 3 post O157:H7 infection, BALB/c mice showed normal values (Fig. 2A).

Leukocytosis and neutrophilia are two phenomena associated with EHEC infections and HUS progression in humans and mice (18–20). Although both mouse strains showed similar numbers of total leukocytes in peripheral blood (Fig. 2B), BALB/c mice showed an increased percentage of circulating neutrophils (% polymorphonuclear leukocytes [PMN]) compared to their own controls and C57 infected mice at day 3 p.i. Infected C57 mice did not show differences compared to their controls (Fig. 2C). We conclude that the increase in circulating PMN after infection may reflect the immune and inflammatory response throughout the infection course.

As expected, control mice from both strains showed a partial weight loss after weaning and starvation (10 to 20%) that was rapidly overcome starting at the second day of the experiments. Infected BALB/c mice showed a delay in weight recovery consistent with lower food consumption compared to control mice up to the third day p.i. (Fig. 2D and F). In contrast, infected C57 mice showed a lower percentage of weight loss during the first days of infection than noninfected mice and also compared to infected BALB/c mice ($P < 0.05$ at day 1; and $P < 0.0001$ at days 2 and 3, C57 versus BALB/c), but afterward they never recovered food intake and their body weight significantly decreased until death (Fig. 2E and G). These data suggest that transient anorexia observed in BALB/c mice was a consequence of weaning and gastrointestinal infection, but perhaps was also important for controlling O157:H7 virulence and sustaining host health during infection. Renal histology at day 3 p.i. confirmed that kidneys from infected C57 mice were severely affected by Stx2a, while BALB/c mice kidneys were relatively conserved. In fact, kidneys from infected C57 mice showed a marked tubular damage with apoptotic cells, a typical injury associated with Stx2 toxicity, while infected BALB/c mice showed only mild damage, mainly vascular congestion and tubular lumen dilation (Fig. 2H).

Survival rates and disease of C57 and BALB/c mice after Stx2a intravenous intoxication. To evaluate if genetic variations were related to Stx2 susceptibility, both mouse strains were intravenously (i.v.) inoculated with a lethal dose of Stx2a (1 ng/ mouse) at weaning.
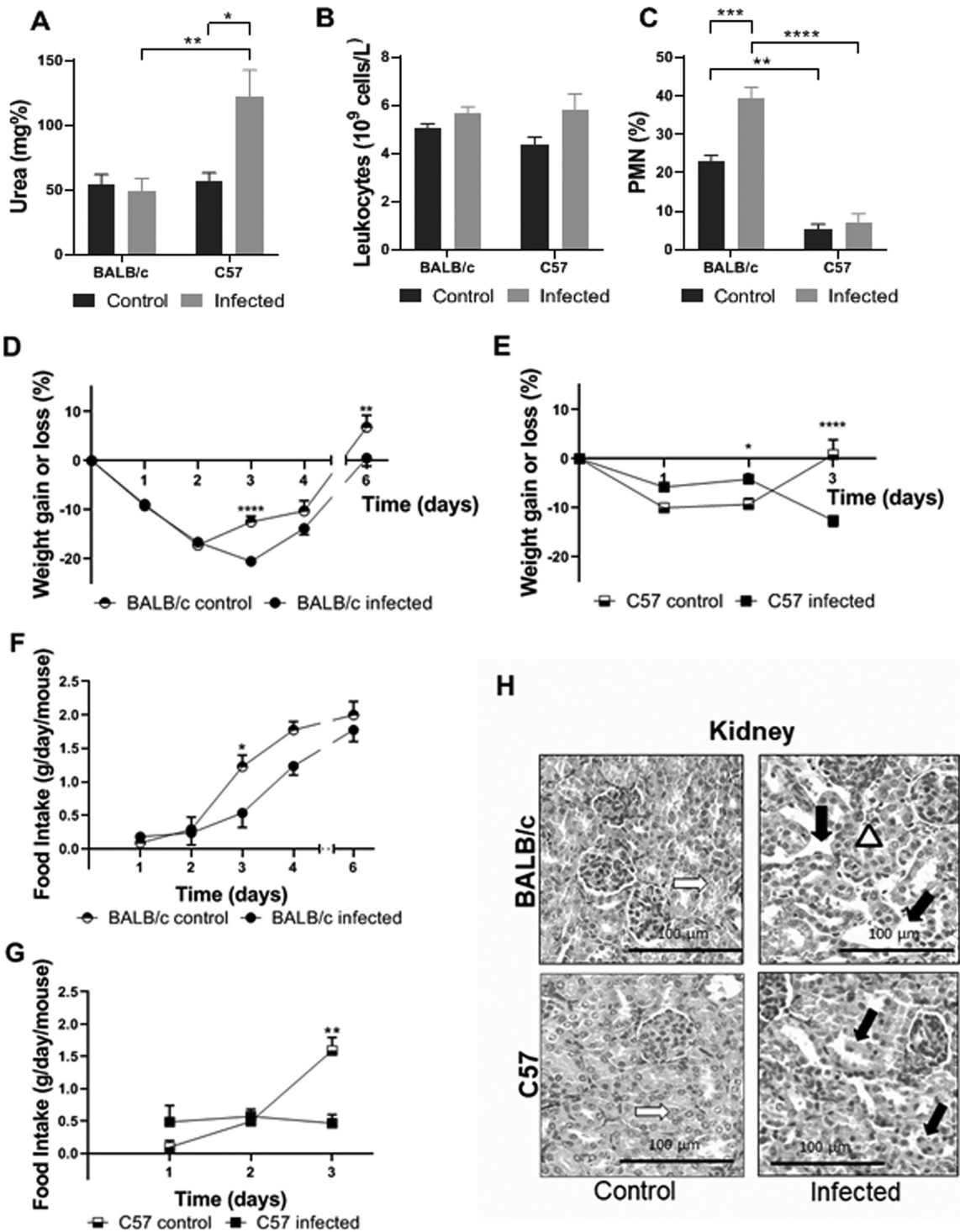
FIG 2 Clinical, biochemical and histological studies during infection with O157:H7. BALB/c and C57 mice were infected with 2 to 3×10^{12} CFU/kg of O157:H7. They were weighed daily and bled at day 3 p.i. The food intake was also recorded daily until the end of the experiments. Each bar or point represents the mean plus the standard error of the mean (mean ± SEM) of 5 mice for the control group and 9 mice for the infected group of each strain. Data from A to G were analyzed by two-way ANOVA test with Tukey's posttest. (A) Plasma urea concentration. (B) Total leukocyte count. (C) Differential PMN count. (D) Percentage of weight gain or loss of BALB/c mice. (E) Percentage of weight gain or loss of C57 mice. (F) Food intake of BALB/c mice. (G) Food intake of C57 mice. *, $P < 0.05$; **, $P < 0.01$; ***, $P < 0.001$; ****, $P < 0.0001$. (H) Kidney histology. Representative images are shown. An infected BALB/c mouse presents vascular congestion in the cortex (white arrowhead) and tubular dilation (black arrows) compared to control. An image from an infected C57 mouse shows areas of tubular necrosis, with loss of epithelium and scaled cells into tubular lumen (black arrows). White arrows show normal tubules from control BALB/c and C57 mice.

Results depicted in Fig. 3A show that BALB/c and C57 mice presented similar survival rates. In correspondence with previous reports (19, 20), all dying mice showed increased plasma urea concentration at day 3 post injection (Fig. 3B) and neutrophilia (Fig. 3C). In addition, BALB/c and C57 mice showed a similar weight loss after Stx2a intoxication, except for two C57 mice that survived (Fig. 3D and E), who reached their body weight a few days after Stx2a injection. The fact that both mouse strains presented a similar pathological response to i.v. Stx2a strongly suggests that genetic differences between these mouse strains have impacts on the susceptibility to O157:H7 infection rather than to Stx2 susceptibility.

O157:H7 burden in the intestine of infected C57 and BALB/c mice. As intestinal colonization is the first step in the pathogenic cascade that leads to systemic illness, we analyzed the level of O157:H7 intestinal colonization versus the infective dose for both mouse strains. O157:H7 CFU recovered from cecum, small intestine, and large intestine of BALB/c mice at day 3 p.i. showed a positive correlation with the inoculum in the three intestinal segments ($r = 0.65$, $P < 0.05$; $r = 0.90$, $P < 0.001$; and $r = 0.84$, $P < 0.01$, respectively). Positive correlations were also observed in the three intestinal segments from C57 mice ($r = 0.88$, $P < 0.01$; $r = 0.89$, $P < 0.01$; and $r = 0.76$, $P < 0.05$, respectively). In addition, the slope of the lines obtained by linear regression for each segment was not statistically different between mouse strains, showing a similar level of colonization at the same O157:H7 infective dose. Also, there was no preferential site of colonization within the same strain.

We conclude that there were no significant differences in the pathogen burden after infection between C57 and BALB/c mice (Fig. 4A to F).

When we evaluated the O157:H7 excretion level, we found a positive correlation between the number of CFU in feces at day 3 p.i. and the inoculum in both mouse strains (BALB/c: $r = 0.93$, $P < 0.01$; C57: $r = 0.90$, $P < 0.01$). Moreover, the slope of the lines obtained by linear regression was not significantly different between C57 and BALB/c mice, suggesting that similar levels of pathogenic bacteria were excreted when they were infected with the same O157:H7 dose (Fig. 4G and H). These data indicate that BALB/c mice remained healthy during infection despite an intestinal colonization level similar to C57 mice.

Histological changes in the intestine of C57 and BALB/c mice after O157:H7 infection. The small and large intestines from C57 and BALB/c mice were histologically analyzed in noninfectious conditions (control) and after 3 days of infection with O157:H7. As observed in Fig. 5, the intestines from control C57 and BALB/c mice did not show pathological alterations. Small and large intestines from infected BALB/c mice showed slight inflammation evidenced by vascular congestion (Fig. 5A). On the other hand, infected C57 mice showed a significant depletion of goblet cells, increased mucosal leukocyte infiltration, and vascular congestion in both intestinal segments. In addition, infected C57 mice showed extended areas of epithelium disruption along the large intestine at day 3 p.i. (Fig. 5A). Taken together, these results indicate BALB/c mice had less intestinal tissue damage and minor inflammation compared to infected C57 mice, despite a similar level of O157:H7 intestinal colonization. It remains unknown whether this observation was a direct consequence of an increased bacterial damage or a deregulated or exacerbated inflammatory response in C57 compared to BALB/c mice.

Intestinal barrier function of C57 and BALB/c mice after O157:H7 infection. Colonization of the intestinal epithelium with O157:H7 causes intestinal damage, inflammation, and increased permeability to and translocation of toxins, of which LPS and Stx are the most pathogenic. Using a fluorescein isothiocyanate-conjugated dextran (FITC-Dx) assay, we found that infected C57 and BALB/c mice showed a higher level of FITC-Dx in serum compared to their corresponding noninfected control group at day 3 p.i. However, infected C57 mice showed a significantly higher FITC-Dx level in serum compared to infected BALB/c mice (Fig. 6). These data indicate that BALB/c mice had reduced damage in the intestinal barrier function induced by O157:H7 infection compared to C57 mice.

Local IgA response in C57 and BALB/c mice during O157:H7 infection. Next, we wondered whether a dissimilar local antibody response between these mouse strains could account for the different outcomes observed during O157:H7 infection. We analyzed
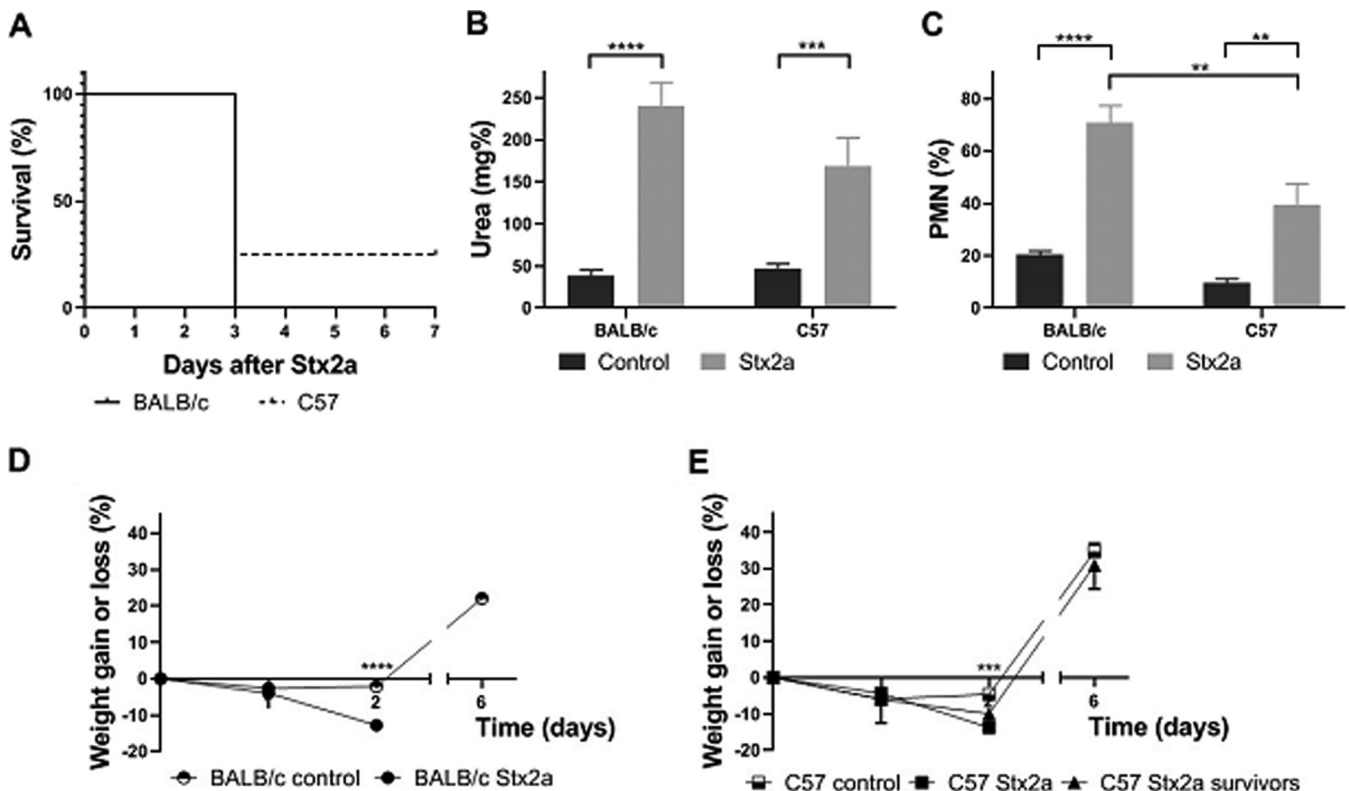
FIG 3 Susceptibility to Stx2a i.v. injection. Eight mice of each strain were challenged with Stx2a (1 ng/mouse) or PBS (control) ($n = 5$ of each strain) at weaning. They were weighed and observed daily and bled at the third day. (A) Survival curve. (B) Plasma urea concentration. (C) Differential count of PMN. (D) Percentage of weight gain or loss of BALB/c mice. (E) Percentage of weight gain or loss of C57 mice. (B to E) Data were analyzed by two-way ANOVA test with Tukey's posttest (**, $P < 0.01$; ***, $P < 0.001$; ****, $P < 0.0001$). (E) ***, $P < 0.001$; compared to Stx2a-injected nonsurviving C57 mice.

the presence of specific antibodies in feces by enzyme-linked immunosorbent assay (ELISA) and flow cytometry. Fecal supernatants from noninfected (control) BALB/c or C57 mice were not able to bind to O157:H7 on ELISA plates (Fig. 7A). Although free anti-O157:H7 IgA was also undetectable in supernatants from infected mice of both strains as soon as 3 days p.i. by ELISA (Fig. 7A), IgA-coated bacteria were detected only in fecal pellets from infected BALB/c mice by flow cytometry (Fig. 7C to E). These results suggest that infection with O157:H7 stimulated the production of local IgA, which was excreted attached to bacteria in feces from BALB/c but not from C57 mice. In line with these results, free anti-O157:H7 IgA was detected in fecal supernatants from all surviving BALB/c mice at day 7 p.i., when no pathogenic bacteria remained in the intestines of mice (Fig. 7B). On the other hand, no C57 mice survived at day 7 p.i. According to the increased survival observed during O157:H7 infection, these results confirmed that only BALB/c mice were able to mount a specific and early local humoral response.

Systemic anti-Stx2 antibody response in C57 and BALB/c mice after O157:H7 infection. We then analyzed if these two mouse strains were able to mount a systemic anti-Stx2 humoral response after O157:H7 infection, as it has been demonstrated that these antibodies are protective against Stx2-induced renal damage (15, 21). Mice were bled at day 3 p.i. and anti-Stx2 IgG levels were determined by ELISA in serial dilutions of serum. As shown in Fig. 8A, BALB/c mice presented anti-Stx2 IgG levels where C57 mice did not, given that their absorbance values were similar to those obtained from noninfected BALB/c and C57 mice. Sera from infected BALB/c mice showed higher levels of anti-Stx2 antibodies after 7 days of infection (Fig. 8B). Thus, BALB/c mice were also able to develop a systemic anti-Stx2 antibody response, which could neutralize Stx2 entering systemic circulation during O157:H7 infection.

Protection experiments in infected C57 and BALB/c mice. Results obtained during antibody response measurement suggested that different outcomes observed between
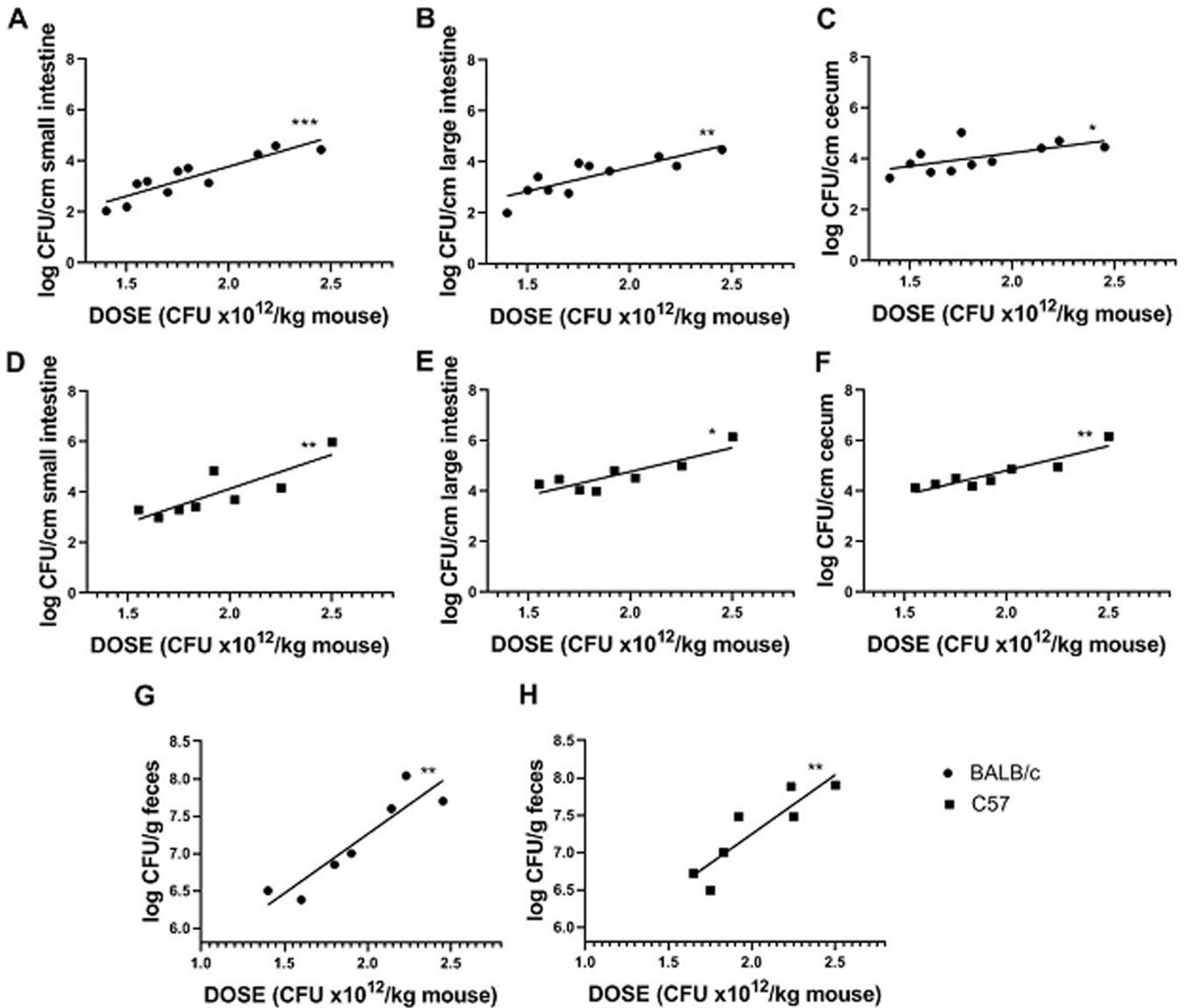
FIG 4 Colonization and bacterial excretion in C57 and BALB/c mice. Eleven BALB/c mice and eight C57 mice were euthanized at day 3 p.i. to determine colonization in the cecum, small intestine, and large intestine. The stools of 7 BALB/c and 7 C57 mice were removed from the large intestine to determine the bacterial excretion. The graphs represent the CFU of O157:H7/cm of intestinal segment or the CFU of O157:H7/g of feces versus the bacterial dose administered as CFU $\times$ 10^{12}/kg. (A to C) Colonization of the small intestine (A), large intestine (B), and cecum (C) from infected BALB/c mice. (D to F) Colonization of the small intestine (D), large intestine (E), and cecum (F) from infected C57 mice. (G and H) Bacterial excretion by infected BALB/c mice (G) and infected C57 mice (H). Data were analyzed by Spearman's correlation test. All associations (log CFU/cm intestinal segment or log CFU/g feces versus CFU $\times$ 10^{12}/kg) show positive correlations: *, $P < 0.05$; **, $P < 0.01$; ***, $P < 0.001$.

BALB/c and C57 mice after infection probably relied on different kinetics in mounting an effective and protective humoral response. To test if C57 mice would have an outcome similar to infected BALB/c mice in the presence of Stx2-neutralizing antibodies, weaned C57 mice were infected with a high dose of O157:H7 and immediately after oral gavage mice were administered phosphate-buffered saline (PBS) or neutralizing anti-Stx2 antibodies. Figure 9A shows that while PBS-treated mice were all dead at day 4 p.i., anti-Stx2 treated mice remained alive. In addition, urea levels and weight curves of the antibody-treated group were normal and significantly different from the PBS-treated one (Fig. 9B and C).

Since these results allowed us to associate the better outcome in BALB/c mice with a specific antibody response against Stx2, we conducted two additional and complementary experiments to directly evaluate whether the anti-Stx2 antibody response in BALB/c mice
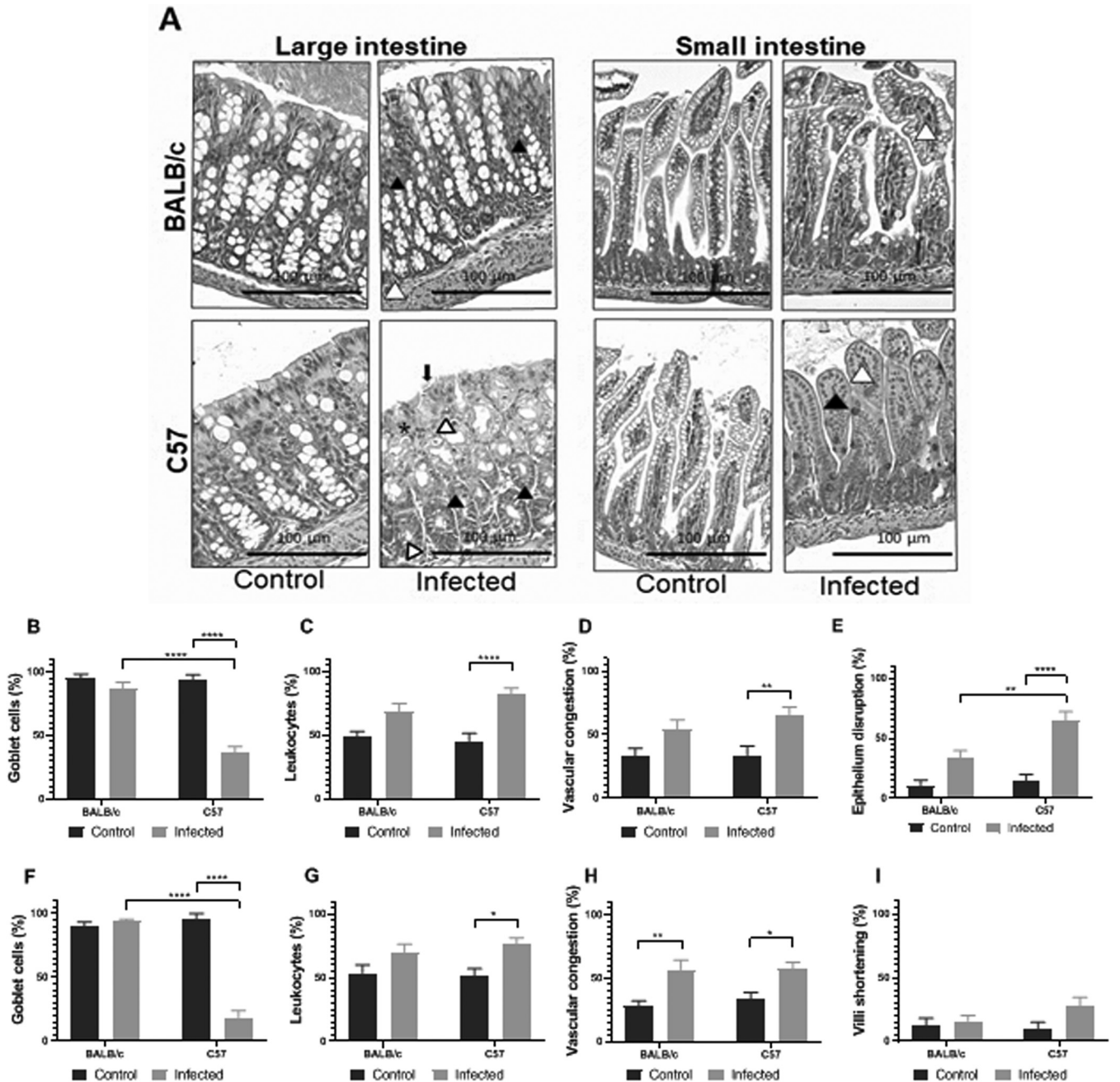
FIG 5 Intestinal histology. Noninfected (control) or infected BALB/c and C57 mice were euthanized at day 3 p.i. and intestines (small and large) were excised. (A). Representative H&E-stained sections from intestinal tissues from BALB/c mice (upper row) or C57 mice (lower row) are shown. Pictures corresponding to the small and the large intestines show vascular congestion (white arrowheads), leukocyte infiltrate (asterisk), foci of goblet cells depletion (black arrowheads), or epithelium disruption (black arrow). Intestinal sections from control mice (BALB/c and C57) show conserved histology. Photos were taken at 200× magnification with bright-field microscopy (Eclipse E-200, Nikon). (B to I) Semiquantification of intestinal damage. Using a grid superimposed on the image, quantification was performed as indicated in the Materials and Methods. The graphs represent the percentage of the fields with at least one goblet cell (B and F), with vascular congestion (C and G), the presence of infiltrated leukocytes (D and H), disrupted epithelium (in large intestine) (E) or the upper third shortening of the villi (small intestine) (I). Three mice were analyzed and showed similar results. Each bar represents the mean ± SEM. Data were analyzed by two-way ANOVA test with Tukey's posttest. Large intestine (B to E): **, $P < 0.01$; ****, $P < 0.0001$. Small intestine (F to I): *, $P < 0.05$; **, $P < 0.01$; ****, $P < 0.0001$.

was responsible for protection against O157:H7 infection. In one experimental schedule, Stx2 toxicity was evaluated in BALB/c mice at day 7 p.i. and compared with toxicity in non-infected litter mates. Both groups of mice were inoculated i.v. with 1 ng of Stx2a, and mortality rates and urea levels were measured at day 3 post intoxication. As can be observed
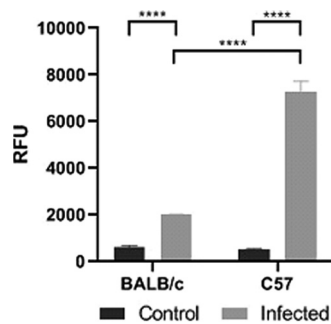
FIG 6 Intestinal permeability. BALB/c and C57 mice received orally 0.1 ml PBS containing FITC-Dx at day 3 p.i. After 4 h of treatment, they were bled to determine relative fluorescence units (RFU) in serum. Each bar shows the mean ± SEM of 3 control and infected mice for each strain. The data were analyzed by two-way ANOVA test with Tukey's posttest: ****, $P < 0.0001$.

in Table 1, infected BALB/c mice were completely protected, remaining alive and showing urea levels significantly lower than the noninfected litter mates.

In a second approach, sera from infected BALB/c mice obtained at day 7 p.i. were transferred to C57 mice by two intraperitoneal (i.p.) injections, at 2 and 24 h after infection. The control group received the same injections of sera from noninfected BALB/c mice. Table 1 shows that sera from infected BALB/c mice were able to confer protection to C57 mice after O157:H7 infection. These results demonstrate that the antibody production by infected BALB/c mice was responsible for the protection against the renal damage induced by Stx2a during O157:H7 infection.

DISCUSSION

EHEC strains belonging to clade 8, which frequently carry $stx2a$ and stx_{2c} genes, cause an unusual high frequency of HUS cases. However, there is a considerable variability in disease severity even among patients infected with this particular lineage.

To gain insight into the influence of host genetic variability on defining the pathogenic response to EHEC, we studied the host fitness, intestinal colonization, tissue damage, and antibody immune response in two mouse strains, BALB/c and C57, after O157:H7 infection. Here, we showed that genetically distinct mouse strains have a different outcome to intragastrical O157:H7 bacterial infection, but a similar response to i.v.-injected Stx2a. Although similar bacterial counts were excreted in feces and collected from intestines from both mouse strains, C57 mice showed signs of severe tissue damage at the intestinal level while BALB/c mice only showed slight vascular congestion and inflammatory alterations when infected with the same O157:H7 bacterial dose. Moreover, BALB/c mice showed a minor passage of FITC-Dx through the intestinal barrier, while C57 mice showed a significantly increased permeability. The increased intestinal damage and decreased barrier function in C57 compared to BALB/c mice probably allowed the passage of pathogenic factors such as LPS and Stx2, which led to renal damage and death, despite a similar level of intestinal colonization in both mouse strains.

When clinical parameters were recorded to follow the infection progression in mice, an increased neutrophilia was observed in BALB/c compared to C57 mice.

The interpretation of this result is not clear. On one hand, control BALB/c in the infection model showed an increased %PMN compared to control C57 mice (Fig. 2), but it was not observed in the Stx2a-intoxication model (Fig. 3). This suggests that the difference could be related to experimental conditions and the response to stressors and/or food privation, instead of being a real difference between strains.

Further, the absence of neutrophilia in C57 mice in the infection model was not observed in the Stx2a-intoxication model, in which both strains showed a similar neutrophilia. Thus, we conclude that neutrophilia during O157:H7 infection in BALB/c mice
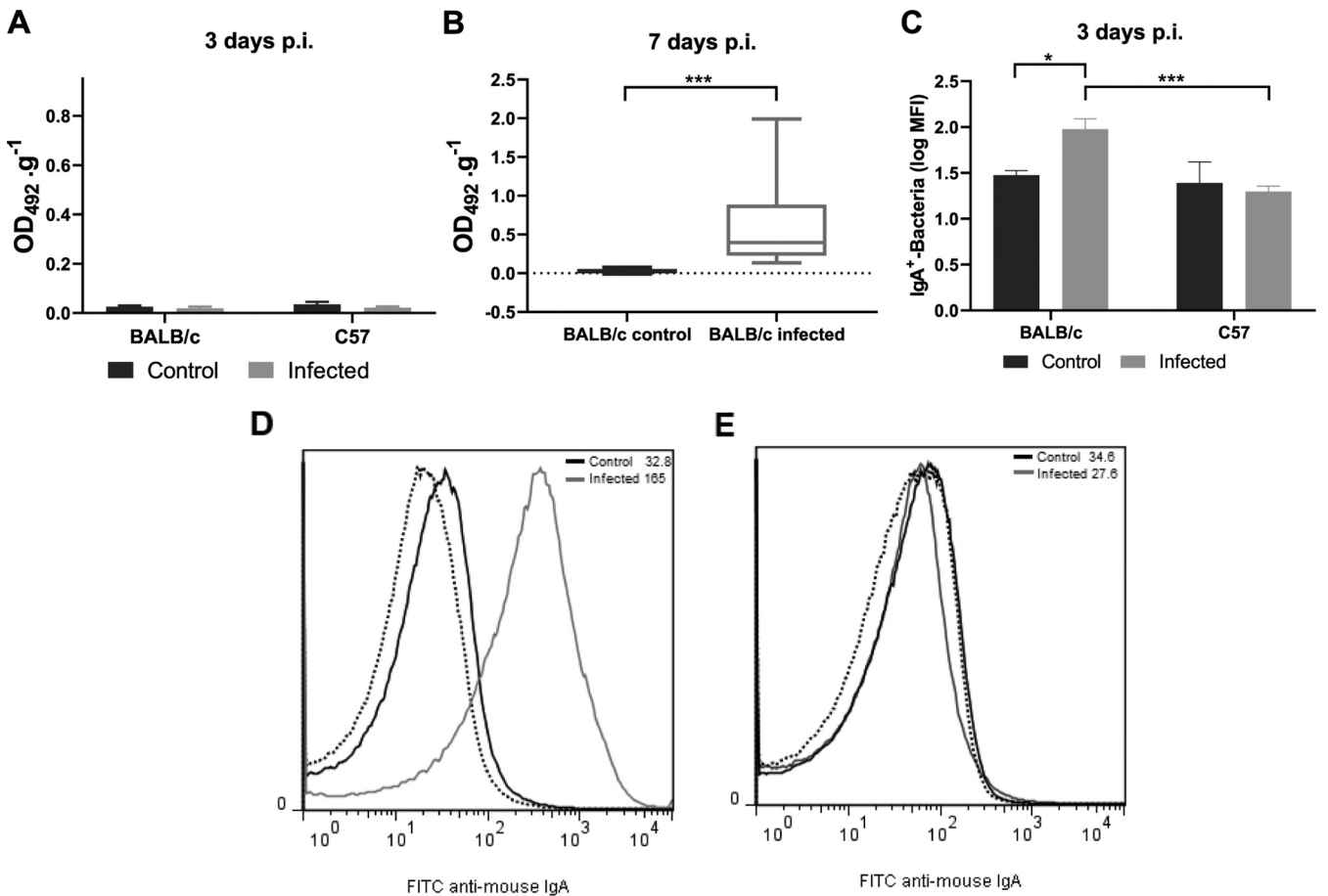
FIG 7 Local humoral response during O157:H7 infection. Contents of the small and large intestine from noninfected (control) or infected mice were prepared as described in the Materials and Methods to determine anti-O157:H7 IgA in supernatants (1/2 dilution) by ELISA and IgA-coated bacteria in pellets by flow cytometry. Antibody levels were expressed as $OD_{492} \cdot g^{-1}$. (A) Free anti-O157:H7 IgA in fecal supernatants at day 3 p.i. Each bar shows the mean $\pm$ SEM of 4 control mice and 6 infected mice for each mouse strain. (B) Free anti-O157:H7 IgA in fecal supernatants at day 7 p.i. The medians and interquartile ranges of 6 controls and 9 infected BALB/c mice are shown. Mann-Whitney test: ***, $P < 0.001$. (C) IgA-coated bacteria at day 3 p.i. Each bar shows the mean $\pm$ SEM of 4 control and 6 infected mice for each mouse strain. Two-way ANOVA test with Tukey's posttest: *, $P < 0.05$; ***, $P < 0.001$. (D and E) Representative histograms of unstained samples (autofluorescence, dotted lines) and FITC anti-mouse IgA-stained samples from control (black lines) or infected (gray lines) BALB/c (D) and C57 (E) mice, assayed in parallel.

reflected an immune response against the gastrointestinal infection and it was probably not a sufficient condition to induce systemic damage.

In addition, an increased weight loss was observed in BALB/c compared to C57 mice, both in control and infected mice. This could be related to how this strain responded to food restriction but not to sickness, because it was transient and rapidly reversed after a maximal weight loss at day 3 p.i., which also correlated with the lowest food intake. In contrast, C57 also showed a maximal weight loss and the lowest food intake at day 3 p.i., but these animals did not survive. Thus, although anorexia and weight loss are related to health conditions, it did not correlate with severity of O157:H7 infection. On the other hand, whether sickness-induced anorexia is beneficial to the host is largely dependent on how the fasted state functionally influences host resistance and tolerance, along with pathogen fitness (22, 23).

In conclusion, both models analyzed together support the concept that an increased neutrophilia and anorexia in BALB/c mice after infection are complex phenomena that could be related to the inflammatory, immune, and/or stress response triggered by intestinal infection and confirm that differences in renal damage and mortality after infection were not related to a differential susceptibility to the toxin activity.

Traditionally, the defense response in animals against microbes has been attributed primarily to the immune response, whose primary function is to sense and eradicate microbes through the participation of microbial killing pathways, collectively referred to as
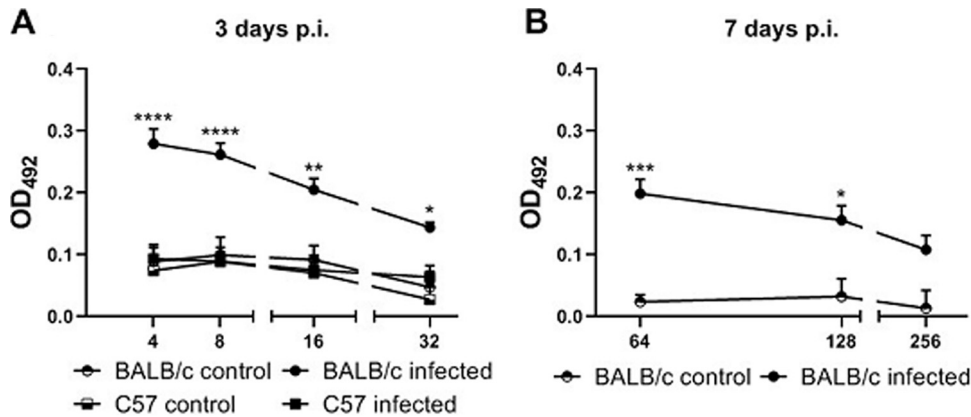
FIG 8 Systemic humoral response during infection with O157:H7. Anti-Stx2B IgG levels were determined in serum from BALB/c and C57 mice at day 3 p.i. and from surviving BALB/c mice at day 7 p.i. by ELISA. Antibody levels were expressed as OD_{492}. The data were analyzed by two-way ANOVA test with Tukey's posttest. (A) Stx2B-specific IgG in serum at day 3 p.i. Each point shows the mean ± SEM of 3 control mice and 8 infected mice for each strain. *, $P < 0.05$; **, $P < 0.01$; ****, $P < 0.0001$ compared to infected C57 and BALB/c control mice at the same dilution. (B) Stx2B-specific IgG in serum from BALB/c mice at day 7 p.i. Each point shows the mean ± SEM of 3 mice for the control group and 8 mice for the infected group. *, $P < 0.05$; ***, $P < 0.001$ compared to the control group at the same dilution.

"resistance mechanisms." However, BALB/c mice maintained their healthy condition in the primary tissues of infection without killing the pathogen, indicating that genetic or epigenetic factors may induce antivirulence mechanisms known as "tolerance mechanisms" to disease, at least at the tested infective doses. Both mouse strains showed similar levels of intestinal colonization and pathogen excretion in the range of O157:H7 infective doses tested, suggesting that both mouse strains were equally resistant to O157:H7. However, C57 mice showed increased tissue damage with a worse outcome than BALB/c mice. Thus, we propose that BALB/c mice are more tolerant to O157:H7 infection than C57 mice. It has been previously demonstrated that an inflammatory immune response is a promising mechanism for limiting infection (11, 22, 23), but also has a high potential to damage host tissues when it is exacerbated or it is not appropriate. Further research is necessary to define if the increased tissue damage observed in C57 mice was caused directly by the pathogen or indirectly by the host immune response.

In this regard, other authors have shown that C57 mice are more likely to develop inflammatory colitis compared to BALB/c mice and require lower doses of dextran sulfate sodium (DSS) to induce a comparable disease severity (24–28). The basis of this
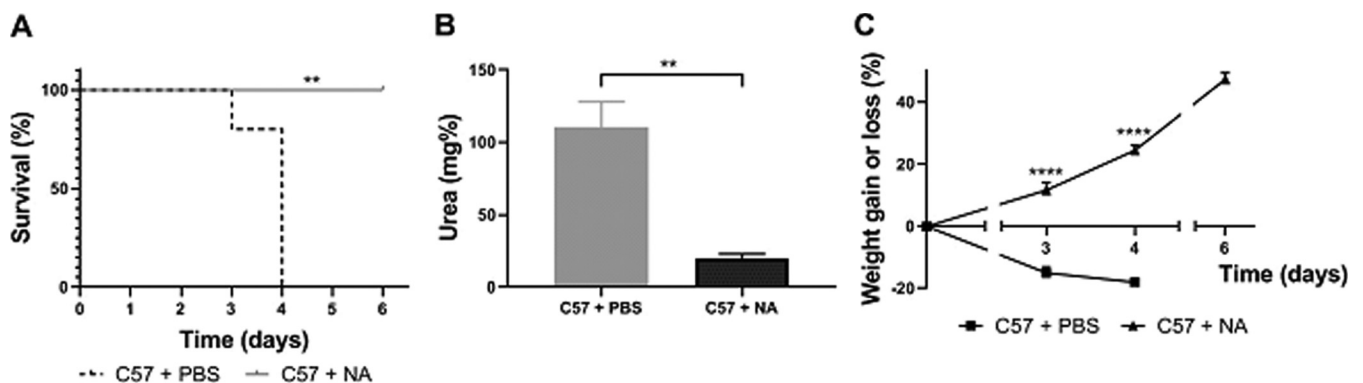

FIG 9 Administration of Stx2-neutralizing antibody to C57-infected mice. Immediately after infection, C57 mice were randomly administered i.v. with PBS or neutralizing anti-Stx2 antibody (NA; 30 pmol). Mice were weighed daily and bled at day 3 p.i. to determine the plasma urea concentration. (A) Survival rates. The data were analyzed by log rank test: **, $P < 0.01$. (B and C) Each point or bar shows the mean ± SEM of 4 mice for each experimental group. (B) Plasma urea levels. The data were analyzed by Student's t parametric test: **, $P < 0.01$. (C) Percent weight gain or loss of PBS and NA-treated mice. The data were analyzed by two-way ANOVA test with Tukey's posttest: ****, $P < 0.0001$ compared to PBS-treated mice at the same day.

TABLE 1 *In vivo* toxin neutralization and C57 protection by transferring BALB/c sera[a]

Groups	Treatment	Mortality rate (dead/total)	Urea (median ± SEM; mg%)
BALB/c control	Stx2a i.v.	5/5	326 ± 71
BALB/c infected	Stx2a i.v.	0/3[b]	92 ± 26[c]
C57 infected	BALB/c control sera	3/3	175 ± 21
C57 infected	BALB/c infected sera	0/3[b]	106 ± 11[c]

[a]Control and infected BALB/c mice received 1 ng of Stx2a by intravenous (i.v) injection at day 7 p.i. C57 mice were i.p. injected with sera from noninfected (control) or infected BALB/c after infection, as detailed in the Materials and Methods. Mortality rate (dead/total) and plasma urea levels (mg%) at day 3 post Stx2a injection (for BALB/c experiments) or at day 3 p.i. (for C57 experiments) are shown.
[b]Significantly different by log rank test ($P < 0.05$) compared with the respective control group.
[c]Significantly different by Student's *t* test ($P < 0.05$) compared with the respective control group.

difference has been attributed to the Th1-Th2 immune balance in these mice, given that BALB/c mice are known as prototypical Th2-type mice, while C57 mice show a more Th1-driven response. However, other authors have demonstrated that severity of acute colitis may be due to the direct cytotoxicity of DSS on epithelial cells and that functional lymphocytes are not involved in this process (28).

Recently, it has been proposed that BALB/c mice exhibit a more efficient mucosal immune system compared to C57 mice as a consequence of better retinoic acid (RA)-mediated signaling (29). It is known that RA favors homing of T regulatory lymphocytes to the intestine (30, 31), improves epithelial integrity, and, thus, increases the intestinal barrier function. In addition, RA affects innate lymphoid cells (ILCs) driving the response toward interleukin 22 (IL-22)-producing group 3 ILCs, which protect against mucosal-associated pathologies. In the same line of findings, it has been recently reported that BALB/c mice have a noticeable amount of innate secretory IgA independent of microbiota colonization. This could be associated with the abundance of B cells, particularly the B1a subtype, in this mouse strain compared to C57 mice (32).

In our experimental approach, none of the noninfected BALB/c or C57 mice showed significant amounts of free innate or polyreactive IgA that cross-reacted with O157:H7 in the intestinal contents assayed by ELISA, nor a significant amount of IgA-coated bacteria determined by flow cytometry. This observation suggests that the local anti-O157:H7 IgA found in infected BALB/c mice was the consequence of a specific immune response. Although polyreactive IgA did not bind to O157:H7, this IgA could play an immune regulatory role in triggering the anti-O157:H7 response in BALB/c mice. In this regard, it has been demonstrated that innate IgA at the intestinal environment plays an important role in controlling *Salmonella enterica* serovar Typhimurium infection and in achieving a better outcome in BALB/c than C57 mice (33). In addition, IgA-coated bacteria were exclusively detected in the pellet fraction of intestinal contents from BALB/c mice at day 3 p.i. Afterward, while IgA-coated bacteria were not detected in the intestinal content from infected BALB/c mice (7 days p.i., data not shown), levels of anti-O157:H7 IgA were found in fecal supernatants. Altogether these results confirm the specificity of the IgA response and indicate that when pathogenic O157:H7 was absent, specific IgA was free and detectable in fecal supernatants. These results suggest that an early stimulation of local IgA production during the infection course was triggered in BALB/c mice but not in C57 mice. Besides the exclusion function, IgA has been shown to allow the limited entrance of IgA-antigen immune complexes or IgA-coated bacteria into Peyer's patches (34–36), favoring the triggering of specific local and systemic immune responses.

In addition, BALB/c mice were able to produce detectable levels of anti-Stx2 IgG in serum as soon as 3 days p.i., while C57 mice did not. As the Stx2 amount necessary to induce renal damage is very low, it has been demonstrated that low concentrations of neutralizing antibodies are able to protect mice against systemic injury (15, 21). In this regard, we demonstrated that a very small quantity of neutralizing anti-Stx2 antibodies i.v. injected into C57

mice immediately after infection were able to completely counteract their death, which clearly depended on Stx2 entering systemic circulation. Furthermore, BALB/c mice that survived O157:H7 infection were protected against the Stx2a challenge, and protection of C57 mice against O157:H7 infection was achieved by transferring serum from infected BALB/c mice.

In summary, an early and specific antibody response mounted in BALB/c mice against pathogenic factors was responsible for their better outcome compared to C57 mice after O157:H7 infection.

The critical role of local antibacterial antibodies and/or serum anti-Stx2 antibodies to contain EHEC intestinal infections in humans has been proposed. In fact, the presence of neutralizing anti-Stx2 antibodies in serum of two resistant human populations, such as recovered HUS-patients and adults from areas of endemicity, constitutes indirect evidence for the correlation between the specific antibody response and protection against systemic complications secondary to EHEC infections (37–39). In addition, an anti-EHEC vaccine for children under 11 years old led to a diminished incidence of HUS (40).

In conclusion, we demonstrated that BALB/c mice present a better outcome secondary to O157:H7 infection through the activation of a tolerance mechanism mainly based on an early and efficient antibody response.

MATERIALS AND METHODS

Mice. BALB/c and C57BL/6 mice (indistinct sex) were purchased from the Charles River Laboratory and maintained in specific-pathogen-free (SPF) conditions at the animal facility of the IMEX-CONICET-Academia Nacional de Medicina, Buenos Aires, Argentina. Mice were housed in standard polypropylene transparent cages under environmentally controlled conditions (temperature, $24 \pm 2°C$; humidity, $50\% \pm 10\%$) with a 12 h light:12 h dark cycle.

Ethical statement. All procedures were approved by the Institutional Animal Care and Use Committee at IMEX-CONICET in accordance with the principles set forth in the Guide for the Care and Use of Laboratory Animals (41) (protocol number 58/2018). Health and behavior of mice were assessed twice a day. Any unnecessary pain, discomfort, or injury to animals was avoided. Mice becoming moribund were humanely euthanized by cervical dislocation. Institutional Animal Care and Use Committee (IACUC) guidelines were used to define humane endpoints.

Bacterial strains and bacterial culture for mice infection. The enterohemorrhagic E. coli strain used in this study was isolated from a fecal specimen of a patient with HUS. This strain belongs to the serotype O157:H7 and clade 8 (9, 14) and harbors the eae, $ehxA$, and stx_{2a} genes, but not stx_1 (14). It also has the Stx2 phage inserted in the $yehV$ site (9), a high Stx2a activity measured on Vero cells in vitro, and a high toxicity in vivo (14).

For preparation of O157:H7 stocks for infection, single colonies that were streaked on LB agar plates were grown in tryptic soy broth (TSB) (Difco, Le Point de Claix, France) in a 37°C shaker until the culture reached the exponential phase. Then, 0.5 ml of this culture was transferred to an Erlenmeyer flask containing 50 ml TSB and incubated overnight in a 37°C shaker. The culture was centrifuged for 30 min at 2,000 rpm, then the bacterial pellet was washed three times and resuspended in sterile PBS to obtain an optimal dose ranging from 1.0×10^{11} to 3.5×10^{11} CFU/ml.

The dose was adjusted by measuring the optical density at 600 nm (OD_{600}) of the bacterial suspension (diluted 1/100 ~0.750 to 1.100 OD units) and interpolating it in a standard curve (OD_{600} versus CFU/ml) performed with the same O157:H7 strain used for infection. Inoculums were confirmed for every experiment by plating dilutions on LB agar plates and quantifying CFU.

Mouse models. Infection protocol: For infection experiments, mice were withheld from feeding for 4 h immediately after weaning (17 to 19 days of age; 6 to 10 g of body weight) and then gavaged with 0.1 ml of bacterial suspension by using a stainless steel cannula (model 7.7.1; 0.38 mm × 22G, Harvard Apparatus, USA), as previously described (14). Control animals received the same volume of sterile PBS. All subsequent assays were performed at day 3 postinfection (p.i.), as this is a critical time in which C57 mice start to die.

Stx2a toxicity assays: For experiments in which Stx2-dependent specific effects were analyzed, Stx2a was prepared as described previously (15). A volume of 0.1 ml sterile PBS containing 1 ng of Stx2a was injected intravenously (i.v.) into the retro-orbital plexus of isoflurane-anesthetized mice. Control mice receiving this dose die 3 to 4 days post injection. The same batch and dose of Stx2a was used for all experiments. The control group received the same volume of sterile PBS.

Anti-Stx2 antibody protection assays: C57 mice were randomly separated in two groups immediately after infection with a high dose of O157:H7. One group of isoflurane-anesthetized mice received an i.v. injection of 0.1 ml containing sterile PBS into the retro-orbital plexus and the other group received a single i.v. dose of 0.1 ml containing an anti-Stx2 neutralizing antibody (30 pmol/mouse), which was prepared and tested in the laboratory (21).

To test toxin neutralization in vivo, infected BALB/c mice received 1 ng of Stx2a at 7 days p.i. as described above. Some noninfected litter mates (control group) received in parallel the same Stx2a dose.

Serum transfer in vivo assays: Infected or noninfected (control) BALB/c mice were bled at day 7 p.i. and the serum was isolated and stored at −20°C until use. To test the protective capacity of these

sera, C57 mice were randomly separated into two groups immediately after infection with a high dose of O157:H7. One group of mice received two intraperitoneal (i.p.) injections of 0.2 ml serum from BALB/c infected mice (1/5 dilution) at 2 and 24 h p.i. The other group received two i.p. injections of 0.2 ml serum from noninfected control BALB/c mice (1/5 dilution).

Food and water were provided *ad libitum* after infection or Stx2a injection, and the animals were observed daily for activity level. Food intake and body weight were recorded until the end of the experiments, when survivors were euthanized. The body weight was expressed as the percentage of weight gain or loss with respect to the initial value. Food consumption per mouse was calculated as the difference in food weight between consecutive days and considering the number of animals in each cage. Blood samples were obtained by puncturing the submandibular plexus at day 3 after bacterial inoculation or Stx2 injection to analyze total and differential blood lymphocytes in a hematologic counter (Abacus Junior Vet, Diatron, USA) and plasma urea levels by a commercial kit (WienerLab, Argentina) following the manufacturer's instructions. Urea levels were expressed as mg urea per 100 ml serum (mg%).

Colonization and bacteria shedding. Mice of each strain were euthanized at day 3 post bacterial inoculation to determine intestinal colonization as previously described (14). Briefly, 5 cm of each intestinal segment and the cecum were removed, washed, and homogenized separately in 0.5 ml sterile PBS. The stools were removed from the large intestine and diluted to a concentration of 0.1 g/ml in sterile PBS. CFU were determined by plating dilutions of the homogenized intestinal tissues and the stools onto MacConkey agar plates and incubating for 16 h at 37°C. Non-sorbitol-fermenting colonies were counted and selected at random for confirmation by multiplex PCR to detect stx_1, stx_2, and *rfbo157* genes using the primers described by Leotta et al. (42). The number of CFU per intestinal segment was calculated by considering the CFU per milliliter and the total volume of each homogenized tissue.

Histological analysis. To assess histological alterations, three randomly selected mice from each experimental group were euthanized 3 days p.i. and kidney and intestines were excised. Samples of these tissues were fixed in 4% formaldehyde, embedded in paraffin, and stained with hematoxylin and eosin (H&E Muto Pure Chemicals, Japan). Images were acquired using brightfield microscopy (Eclipse E-200, Nikon). Kidney damage was shown mainly by tubular necrosis. Intestinal damage was evidenced by the following parameters: depletion of goblet cells, presence of vascular congestion, infiltrating leukocytes, and epithelium disruption for large intestines or the shortening of the upper third of the villi for small intestines. Ten separated fields of each tissue were scanned at 200× magnification. Using a grid superimposed on the images, quantification was performed on 90 fields of each histological preparation with ImageProPlus 6 software (Image Pro Plus 6, Media Cybernetics, USA) (43).

Gut permeability assay. To assess the intestinal barrier function, a fluorescein isothiocyanate (FITC)-conjugated dextran (FITC-Dx; mean molecular weight 4 kDa) (Sigma-Aldrich, USA) assay was performed as previously described with modifications (16). A volume of 0.1 ml sterile PBS containing 80 g/liter FITC-Dx was administered by oral gavage after 3 days of O157:H7 infection. The fluorescence of FITC-Dx was measured in serum after 4 h of treatment using a microvolume fluorimeter (Thermo Scientific NanoDrop, USA).

Determination of IgA-coated bacteria by flow cytometry. Feces from small and large intestines were collected and transferred to a tube where they were diluted to 1 g/ml in sterile PBS containing 1 mM phenylmethylsulfonyl fluoride (PBS-PMSF). Each sample was vortexed for 5 min and then centrifuged at 4,500 rpm for 5 min to precipitate debris. Supernatants were collected and then centrifuged at 13,300 rpm for 5 min to precipitate bacteria. The supernatants obtained were stored at −80°C to determine free anti-O157:H7 IgA levels. The pellets were resuspended in PBS-PMSF and incubated with FITC-conjugated rat anti-mouse IgA (BD Biosciences, USA) for 1 h at 4°C sheltered from the light. Then, bacteria pellets were washed by centrifugation at 13,300 rpm, resuspended in 2% paraformaldehyde, and incubated for 30 min at 4°C sheltered from the light. Samples were analyzed by flow cytometry for analysis of IgA-coated bacteria as previously described (44). Samples were acquired immediately on a Becton, Dickinson (BD, Franklin Lakes, NJ, USA) fluorescence activated cell sorter (FACScan). Bacteria were delimited by size and granularity (in a logarithmic scale for forward and side scatter) and 200,000 events were acquired for subsequent analysis using FlowJo 7.6 software.

Determination of free anti-O157:H7 IgA in fecal supernatants by ELISA. The supernatants obtained by centrifugation of feces at 13,300 rpm for 5 min were stored at −80°C to determine anti-O157:H7 IgA levels. These antibodies were analyzed by enzyme-linked immunosorbent assay (ELISA) as previously described (17). Intact formalin-killed O157:H7 were prepared as follows. Bacteria were grown in TSB overnight at 37°C with slow agitation, washed twice with sterile PBS by centrifugation, and resuspended in PBS containing 0.5% neutralized formalin. The bacterial suspension was stored for 3 days at room temperature and then washed twice with sterile PBS to remove free Stx2a. Afterward, 96-well MaxiSorp plates (Greiner Bio-One, Germany) were incubated with the formalin-killed O157:H7 suspension diluted to an OD_{600} of 0.1 per ml of 15 mM carbonate-25 mM bicarbonate buffer (pH 9.6) overnight at 4°C. Wells were washed with 0.05% Tween20 in PBS (PBS-T), blocked with 2% bovine serum albumin (BSA; Sigma-Aldrich, USA) in PBS (PBS-BSA) for 1.5 h at room temperature, washed again with PBS-T, and finally incubated with the fecal supernatants (1/2 dilution) overnight at 4°C. After incubation, wells were washed with PBS-T and incubated with peroxidase-conjugated goat anti-mouse IgA (Chemicon International, USA) diluted (1/2,000) in PBS-BSA for 1.5 h at room temperature with orbital agitation. Plates were washed and the reaction was carried out with 2 mg/ml *o*-phenylenediamine (Sigma-Aldrich, USA) and 0.33% H_2O_2 in 0.1 M citrate-0.2 M phosphate buffer (pH 5.0). The reaction was stopped with 2 M H_2SO_4 and absorbance at 492 nm was measured on an Asys UVM340 microtiter plate reader (Biochrom Ltd., Cambridge, UK). Results were expressed as OD at 492 nm (OD_{492}) units per gram of feces, which represent the value obtained for each sample minus the OD_{492} obtained for its nonspecific binding and considering the dilution made.

Determination of specific anti-Stx2 IgG in serum by ELISA. ELISA was performed as previously described (17, 21). Briefly, 96-well MaxiSorp plates were coated with 5 μg of purified Stx2-B subunit conjugated to histidine per ml 15 mM carbonate-25 mM bicarbonate buffer (pH 9.6) overnight at 4°C and, after washing with PBS-T, blocked with PBS-BSA for 1.5 h at room temperature. Then, the plates were washed with PBS-T and incubated with serially diluted mouse serum overnight at 4°C. After washing, plates were incubated with peroxidase-conjugated goat anti-mouse IgG (Chemicon International, USA) diluted (1/2,000) in PBS-BSA for 1.5 h at room temperature with orbital agitation. Plates were washed and the reaction was developed as described above. Antibody levels were expressed as OD_{492}, which represent the value obtained for each sample minus the OD_{492} obtained for its nonspecific binding.

Statistical analysis. Survival data were analyzed for significance by using a log rank test. Data expressed as the mean $\pm$ standard error of the mean (SEM) were analyzed for statistical differences using Student's t test or a one- or two-way analysis of variance (ANOVA) followed by Tukey's posttest. The assumption of Gaussian distribution (Shapiro-Wilk's test) and heteroscedasticity (Spearman's test) were evaluated. In cases where the raw data did not fulfill these assumptions, a nonparametric Mann-Whitney test was used for comparing two groups, or else log transformation was performed to use the two-way ANOVA followed by a Tukey's posttest. Contingency analysis was done using the Fisher's exact test. Correlations were analyzed with the Spearman's test. Slope comparisons were done using a t test postlinear regression. All data were analyzed by the Prism 8.0 software (GraphPad, United States).

REFERENCES

1. Bruyand M, Mariani-Kurkdjian P, Gouali M, de Valk H, King LA, Le Hello S, Bonacorsi S, Loirat C. 2018. Hemolytic uremic syndrome due to Shiga toxin-producing Escherichia coli infection. Med Mal Infect 48:167–174. https://doi.org/10.1016/j.medmal.2017.09.012.

2. Pianciola L, Rivas M. 2018. Genotypic features of clinical and bovine *Escherichia coli* O157 strains isolated in countries with different associated-disease incidences. Microorganisms 6:36. https://doi.org/10.3390/microorganisms6020036.

3. Ylinen E, Salmenlinna S, Halkilahti J, Jahnukainen T, Korhonen L, Virkkala T, Rimhanen-Finne R, Nuutinen M, Kataja J, Arikoski P, Linkosalo L, Bai X, Matussek A, Jalanko H, Saxén H. 2020. Hemolytic uremic syndrome caused by Shiga toxin-producing Escherichia coli in children: incidence, risk factors, and clinical outcome. Pediatr Nephrol 35:1749–1759. https://doi.org/10.1007/s00467-020-04560-0.

4. Manning SD, Motiwala AS, Springman AC, Qi W, Lacher DW, Ouellette LM, Ouellette LM, Mladonicky JM, Somsel P, Rudrik JT, Dietrich SE, Zhang W, Swaminathan B, Alland D, Whittam TS. 2008. Variation in virulence among clades of *Escherichia coli* O157:H7 associated with disease outbreaks. Proc Natl Acad Sci U S A 105:4868–4873. https://doi.org/10.1073/pnas.0710834105.

5. Sanchez KK, Chen GY, Palaferri Schieber AM, Redford SE, Shokhirev MN, Leblanc M, Lee YM, Ayres JS. 2018. Cooperative metabolic adaptations in the host can favor asymptomatic infection and select for attenuated virulence in an enteric pathogen. Cell 175:146–158. https://doi.org/10.1016/j.cell.2018.07.016.

6. Ebert D, Hamilton WD. 1996. Sex against virulence: the coevolution of parasitic diseases. Trends Ecol Evol 11:79–82. https://doi.org/10.1016/0169-5347(96)81047-0.

7. Woolhouse ME, Webster JP, Domingo E, Charlesworth B, Levin BR. 2002. Biological and biomedical implications of the co-evolution of pathogens and their hosts. Nat Genet 32:569–577. https://doi.org/10.1038/ng1202-569.

8. Lambrechts L, Fellous S, Koella JC. 2006. Coevolutionary interactions between host and parasite genotypes. Trends Parasitol 22:12–16. https://doi.org/10.1016/j.pt.2005.11.008.

9. Amigo N, Mercado E, Bentancor A, Singh P, Vilte D, Gerhardt E, Zotta E, Ibarra C, Manning SD, Larzábal M, Cataldi A. 2015. Clade 8 and clade 6 strains of

Escherichia coli O157:H7 from cattle in Argentina have hypervirulent-like phenotypes. PLoS One 10:e0127710. https://doi.org/10.1371/journal.pone.0127710.

10. Iyoda S, Manning SD, Seto K, Kimata K, Isobe J, Etoh Y, Ichihara S, Migita Y, Ogata K, Honda M, Kubota T, Kawano K, Matsumoto K, Kudaka J, Asai N, Yabata J, Tominaga K, Terajima J, Morita-Ishihara T, Izumiya H, Ogura Y, Saitoh T, Iguchi A, Kobayashi H, Hara-Kudo Y, Ohnishi M, Arai R, Kawase M, Asano Y, Asoshima N, Chiba K, Furukawa I, Kuroki T, Hamada M, Harada S, Hatakeyama T, Hirochi T, Sakamoto Y, Hiroi M, Takashi K, Horikawa K, Iwabuchi K, Kameyama M, Kasahara H, Kawanishi S, Kikuchi K, Ueno H, Kitahashi T, Kojima Y, Konishi N, . 2014. Phylogenetic clades 6 and 8 of enterohemorrhagic Escherichia coli O157:H7 with particular stx subtypes are more frequently found in isolates from hemolytic uremic syndrome patients than from asymptomatic carriers. Open Forum Infect Dis 1:ofu061. https://doi.org/10.1093/ofid/ofu061.

11. Rausher MD. 2001. Co-evolution and plant resistance to natural enemies. Nature 411:857–864. https://doi.org/10.1038/35081193.

12. Råberg L, Sim D, Read AF. 2007. Disentangling genetic variation for resistance and tolerance to infectious diseases in animals. Science 318:812–814. https://doi.org/10.1126/science.1148526.

13. Restif O, Koella JC. 2004. Concurrent evolution of resistance and tolerance to pathogens. Am Nat 164:E90–102. https://doi.org/10.1086/423713.

14. Brando RJF, Miliwebsky E, Bentancor L, Deza N, Baschkier A, Ramos MV, Fernández GC, Meiss R, Rivas M, Palermo MS. 2008. Renal damage and death in weaned mice after oral infection with Shiga toxin 2-producing *Escherichia coli* strains. Clin Exp Immunol 153:297–306. https://doi.org/10.1111/j.1365-2249.2008.03698.x.

15. Mejías MP, Hiriart Y, Lauché C, Fernández-Brando RJ, Pardo R, Bruballa A, Ramos MV, Goldbaum FA, Palermo MS, Zylberman V. 2016. Development of camelid single chain antibodies against Shiga toxin type 2 (Stx2) with therapeutic potential against Hemolytic Uremic Syndrome (HUS). Sci Rep 6:24913. https://doi.org/10.1038/srep24913.

16. Cabrera G, Fernández-Brando RJ, Mejías MP, Ramos MV, Abrey-Recalde MJ, Vanzulli S, Vermeulen M, Palermo MS. 2015. Leukotriene C4 increases the susceptibility of adult mice to Shiga toxin-producing *Escherichia coli*

infection. Int J Med Microbiol 305:910–917. https://doi.org/10.1016/j.ijmm.2015.09.006.

17. Mejias MP, Cabrera G, Fernández-Brando RJ, Baschkier A, Ghersi G, Abrey-Recalde MJ, Miliwebsky E, Meiss R, Goldbaum F, Zylberman V, Rivas M, Palermo MS. 2014. Protection of mice against Shiga toxin 2 (Stx2)-associated damage by maternal immunization with a Brucella lumazine synthase-Stx2 B subunit chimera. Infect Immun 82:1491–1499. https://doi.org/10.1128/IAI.00027-14.

18. Dennhardt S, Pirschel W, Wissuwa B, Daniel C, Gunzer F, Lindig S, Medyukhina A, Kiehntopf M, Rudolph WW, Zipfel PF, Gunzer M, Figge MT, Amann K, Coldewey SM. 2018. Modeling hemolytic-uremic syndrome: in-depth characterization of distinct murine models reflecting different features of human disease. Front Immunol 9:1459. https://doi.org/10.3389/fimmu.2018.01459.

19. Ramos MV, Mejias MP, Sabbione F, Fernandez-Brando RJ, Santiago AP, Amaral MM, Exeni R, Trevani AS, Palermo MS. 2016. Induction of neutrophil extracellular traps in Shiga toxin-associated hemolytic uremic syndrome. J Innate Immun 8:400–411. https://doi.org/10.1159/000445770.

20. Cabrera G, Fernández-Brando RJ, Abrey-Recalde MJ, Baschkier A, Pinto A, Goldstein J, Zotta E, Meiss R, Rivas M, Palermo MS. 2014. Retinoid levels influence enterohemorrhagic Escherichia coli infection and Shiga toxin 2 susceptibility in mice. Infect Immun 82:3948–3957. https://doi.org/10.1128/IAI.02191-14.

21. Mejias MP, Ghersi G, Craig PO, Panek CA, Bentancor LV, Baschkier A, Goldbaum FA, Zylberman V, Palermo MS. 2013. Immunization with a chimera consisting of the B subunit of Shiga toxin type 2 and brucella lumazine synthase confers total protection against Shiga toxins in mice. J Immunol 191:2403–2411. https://doi.org/10.4049/jimmunol.1300999.

22. Schneider DS, Ayres JS. 2008. Two ways to survive infection: what resistance and tolerance can teach us about treating infectious diseases. Nat Rev Immunol 8:889–895. https://doi.org/10.1038/nri2432.

23. Medzhitov R, Schneider DS, Soares MP. 2012. Disease tolerance as a defense strategy. Science 335:936–941. https://doi.org/10.1126/science.1214935.

24. Camuesco D, Rodriguez-Cabezas ME, Garrido-Mesa N, Cueto-Sola M, Bailon E, Comalada MB, Arribas B, Merlos M, Balsa D, Zarzuelo A, Janer G, Xaus J, Román J, Gálvez J. 2012. The intestinal anti-inflammatory effect of dersalazine sodium is related to a downregulation in IL-17 production in experimental models of rodent colitis. Br J Pharmacol 165:729–740. https://doi.org/10.1111/j.1476-5381.2011.01598.x.

25. Melgar S, Drmotova M, Rehnstrom E, Jansson L, Michaelsson E. 2006. Local production of chemokines and prostaglandin E-2 in the acute, chronic and recovery phase of murine experimental colitis. Cytokine 35:275–283. https://doi.org/10.1016/j.cyto.2006.09.007.

26. Sasaki S, Ishida Y, Nishio N, Ito S, Isobe K. 2008. Thymic involution correlates with severe ulcerative colitis induced by oral administration of dextran sulphate sodium in C57BL/6 mice but not in BALB/c mice. Inflammation 31:319–328. https://doi.org/10.1007/s10753-008-9081-3.

27. Siegmund B, Fantuzzi G, Rieder F, Gamboni-Robertson F, Lehr HA, Hartmann G, Dinarello CA, Endres S, Eigler A. 2001. Neutralization of interleukin-18 reduces severity in murine colitis and intestinal IFN-gamma and TNF-alpha production. Am J Physiol Regul Integr Comp Physiol 281: R1264–273. https://doi.org/10.1152/ajpregu.2001.281.4.R1264.

28. Tsuchiya T, Fukuda S, Hamada H, Nakamura A, Kohama Y, Ishikawa H, Tsujikawa K, Yamamoto H. 2003. Role of gamma delta T cells in the inflammatory response of experimental colitis mice. J Immunol 171:5507–5513. https://doi.org/10.4049/jimmunol.171.10.5507.

29. Goverse G, Olivier BJ, Molenaar R, Knippenberg M, Greuter M, Konijn T, Cook EC, Beijer MR, Fedor DM, den Haan JM, Napoli JL, Bouma G, Mebius RE. 2015. Vitamin A metabolism and mucosal immune function are distinct between BALB/c and C57BL/6 mice. Eur J Immunol 45:89–100. https://doi.org/10.1002/eji.201343340.

30. Bai A, Lu N, Guo Y, Liu Z, Chen J, Peng Z. 2009. All-trans retinoic acid down regulates inflammatory responses by shifting the Treg/Th17 profile in human ulcerative and murine colitis. J Leukoc Biol 86:959–969. https://doi.org/10.1189/jlb.0109006.

31. Menning A, Loddenkemper C, Westendorf AM, Szilagyi B, Buer J, Siewert C, Hamann A, Huehn J. 2010. Retinoic acid-induced gut tropism improves the protective capacity of Treg in acute but not in chronic gut inflammation. Eur J Immunol 40:2539–2548. https://doi.org/10.1002/eji.200939938.

32. Fransen F, Zagato E, Mazzini E, Fosso B, Manzari C, El Aidy S, Chiavelli A, D'Erchia AM, Sethi MK, Pabst O, Marzano M, Moretti S, Romani L, Penna G, Pesole G, Rescigno M. 2015. BALB/c and C57BL/6 mice differ in polyreactive IgA abundance, which impacts the generation of antigen-specific IgA and microbiota diversity. Immunity 43:527–540. https://doi.org/10.1016/j.immuni.2015.08.011.

33. Wijburg OLC, Uren TK, Simpfendorfer K, Johansen F-E, Brandtzaeg P, Strugnell RA. 2006. Innate secretory antibodies protect against natural Salmonella typhimurium infection. J Exp Med 203:21–26. https://doi.org/10.1084/jem.20052093.

34. Kadaoui KA, Corthésy B. 2007. Secretory IgA mediates bacterial translocation to dendritic cells in mouse Peyer's patches with restriction to mucosal compartment. J Immunol 179:7751–7757. https://doi.org/10.4049/jimmunol.179.11.7751.

35. Martinoli C, Chiavelli A, Rescigno M. 2007. Entry route of Salmonella typhimurium directs the type of induced immune response. Immunity 27:975–984. https://doi.org/10.1016/j.immuni.2007.10.011.

36. Breedveld A, van Egmond M. 2019. IgA and FcαRI: pathological roles and opportunities. Front Immunol 10:553. https://doi.org/10.3389/fimmu.2019.00553.

37. Fernández-Brando RJ, Bentancor LV, Mejías MP, Ramos MV, Exeni A, Exeni C, Laso MC, Exeni R, Isturiz MA, Palermo MS. 2011. Antibody response to Shiga toxins in Argentinean children with enteropathic hemolytic uremic syndrome at acute and long-term follow-up periods. PLoS One 6:e19136. https://doi.org/10.1371/journal.pone.0019136.

38. Ludwig K, Karmali MA, Sarkim V, Bobrowski C, Petric M, Karch H, Müller-Wiefel DE, Arbeitsgemeinschaft für Pädiatrische Nephrologie. 2001. Antibody response to Shiga toxins Stx2 and Stx1 in children with enteropathic hemolytic-uremic syndrome. J Clin Microbiol 39:2272–2279. https://doi.org/10.1128/JCM.39.6.2272-2279.2001.

39. Karmali MA, Mascarenhas M, Petric M, Dutil L, Rahn K, Ludwig K, Arbus GS, Michel P, Sherman PM, Wilson J, Johnson R, Kaper JB. 2003. Age-specific frequencies of antibodies to Escherichia coli verocytotoxins (Shiga toxins) 1 and 2 among urban and rural populations in southern Ontario. J Infect Dis 188:1724–1729. https://doi.org/10.1086/379726.

40. Szu SC, Ahmed A. 2014. Clinical studies of Escherichia coli O157:H7 conjugate vaccines in adults and young children. Microbiol Spectr 2. https://doi.org/10.1128/microbiolspec.EHEC-0016-2013.

41. National Research Council. 2011. Guide for the care and use of laboratory animals, 8th ed National Academies Press, Washington, DC.

42. Leotta GA, Chinen I, Epszteyn S, Miliwebsky E, Melamed IC, Motter M, Ferrer M, Marey E, Rivas M. 2005. Validation of a multiplex PCR for detection of Shiga toxin producing Escherichia coli (in Spanish). Rev Argent Microbiol 37:1–10.

43. Ochoa F, Lago NR, Gerhardt E, Ibarra C, Zotta E. 2010. Characterization of Stx2 tubular response in a rat experimental model of hemolytic uremic syndrome. Am J Nephrol 32:340–346. https://doi.org/10.1159/000319444.

44. Gonçalves Miranda MC, Pires Oliveira R, Torres L, Leão Fiorini Aguiar S, Pinheiro-Rosa N, Lemos L, Guimarães MA, Reis D, Silveira T, Ferreira Ê, Moreira TG, Cara DC, Maioli TU, Kelsall BL, Carlos D, Faria AMC. 2019. Frontline Science: abnormalities in the gut mucosa of non-obese diabetic mice precede the onset of type 1 diabetes. J Leukoc Biol 106:513–529. https://doi.org/10.1002/JLB.3HI0119-024RR.